

# Thermolysis of acidic aluminum chloride solution and its products

Victor V. Ivanov<sup>a</sup>, Sergei D. Kirik<sup>b</sup>, Alexander A. Shubin<sup>a,\*</sup>, Irina A. Blokhina<sup>a</sup>,  
Victor M. Denisov<sup>a</sup>, Lilya A. Irtugo<sup>a</sup>

<sup>a</sup>Siberian Federal University, 79 Svobodny, Krasnoyarsk 660041, Russia

<sup>b</sup>Institute of Chemistry and Chemical Technology SB RAS, 42K. Marx Street, Krasnoyarsk 660049, Russia

Received 12 May 2012; received in revised form 26 September 2012; accepted 18 October 2012

Available online 26 October 2012

## Abstract

A saturated acidic aluminum chloride solution with a total composition of  $\text{AlCl}_3 \cdot \text{HCl} \cdot 12\text{H}_2\text{O}$  was obtained, and its behavior under thermal treatments was studied using thermogravimetry, differential scanning calorimetry and mass spectrometry techniques. The thermolysis solid products were characterized with XRD and SEM. Four stages of the thermolysis could be distinguished. Initially, the solution lost free water molecules, and an amorphous precipitate with an approximate composition  $\text{AlCl}_3 \cdot \text{HCl} \cdot 12\text{H}_2\text{O}$  was obtained as a product. The precipitate released eight water molecules in the temperature range 390–425 K. Then, all chlorine atoms in the form of HCl and two water molecules were outgassed at 425–485 K. The product completely lost water up to 650 K. The crystallization of the solid begins with appearance of the phase  $\gamma\text{-Al}_2\text{O}_3$  at 1073 K, and the final product,  $\alpha\text{-Al}_2\text{O}_3$ , is observed at 1323 K. The application of the saturated trichloride solutions as a binder and a promoter for activated sintering of composite ceramics on the base of alumina was examined.

© 2012 Elsevier Ltd and Techna Group S.r.l. All rights reserved.

**Keywords:** Aluminum chloride; Thermolysis; Thermal analysis; Bonding material

## 1. Introduction

Aluminum trichloride,  $\text{AlCl}_3 \cdot 6\text{H}_2\text{O}$ , and its decomposition products are used as binding activating agents for sintering when preparing widely used ceramics based on aluminum oxide [1]. Salt application is used because it makes it possible to prepare a saturated solution with a high content of aluminum. The solution efficiently penetrates into the pores and covers the surface of the ceramic ingredients, and under thermal treatment, it gives rise to the aluminum oxide, which serves as a binding component. The technical application of the salt is reasonable because of its quite simple synthesis that employs inexpensive reagents. The effective, practical application of the salt requires an understanding of its solutions properties, the processes of thermal decomposition and the characteristics of the thermolysis solid products considered for this purpose. There are some data in the literature on the

thermolysis of aluminum trichloride ( $\text{AlCl}_3 \cdot 6\text{H}_2\text{O}$ ) [1–3]. The aluminum trichloride solution is a weak acid medium. The acidity changes the viscosity and the surface properties of the solution, which eventually influences its penetrability for wetting the microcracks and pores. These properties are very significant for both preparing ceramics and the quality of the resulting ceramics. The adhesion properties and thermal behavior of aluminum trichloride solutions with a high acid content have not been investigated. Therefore, it is believed that these solutions will behave differently. It is well known that the aluminum atoms are coordinated by oxygen in crystals of  $\text{AlCl}_3 \cdot 6\text{H}_2\text{O}$  [4]. The chlorine ions are located in the external coordination sphere. In salts of the apparent superacid  $\text{HAlCl}_4$  [5], such as  $\text{LiAlCl}_4$  [6] and  $\text{NaAlCl}_4$  [7], the aluminum atoms are chemically connected through the chlorine atoms.

Because there is a practical interest in chloride aluminum salt solutions, particularly for manufacturing aluminum wettable  $\text{TiB}_2\text{-Al}_2\text{O}_3$  ceramics for cathodes of aluminum electrolyzers, the thermal behavior of saturated aluminum trichloride acid solutions was investigated in our work.

\*Corresponding author. Tel.: +79050878981.

E-mail address: [Ashubin@sfu-kras.ru](mailto:Ashubin@sfu-kras.ru) (A.A. Shubin).

## 2. Experimental

The aluminum trichloride (ATC) solution was prepared by boiling  $\text{Al}(\text{OH})_3$  (technical aluminum hydroxide, 48–0114–65–91 specification) in a  $\text{HCl}$  solution ( $\sim 36\%$ ). The solution was evaporated to a density of  $1.33 \text{ g/cm}^3$ . Sediment appears after the density exceeds this value.

The pH was measured using an InoLab pH-730 instrument. The thermal decomposition processes were investigated using thermogravimetry (TG), differential scanning calorimetry (DSC) and gas emission mass spectrometry (EMS) during the thermolysis using the synchronous thermal analyzer Netzsch STA 449C combined with an Aëolos QMS 403C mass spectrometer. All processes were performed in a platinum crucible with an argon turning atmosphere (the velocity of the stream was approximately  $10\text{--}25 \text{ ml/min}$ ), and the sample heating rate was  $5 \text{ K/min}$ .

The Al:Cl ratio in the samples was evaluated using X-ray fluorescence with an ARL Advant'X wave dispersive spectrometer. The thermolysis products were characterized using X-ray powder diffraction (XRD) on an X'Pert-Pro (PANalytical) diffractometer with  $\text{Cu K}\alpha$  radiation ( $\lambda_1 = 0.15406 \text{ \AA}$ ,  $\lambda_2 = 0.15444 \text{ \AA}$ ). Diffraction patterns were recorded over an angular range of  $5^\circ\text{--}80^\circ 2\theta$  with a step size of  $0.026^\circ$ . Scanning electronic microscopy (SEM) was used to observe the morphology of the decomposition products. The SEM images were obtained using a JEOL JSM-7001 F instrument (with an accelerating voltage of  $5 \text{ kV}$ ).

IR-analyses were performed on a FTIR spectrometer Nicolet 6700 equipped with DTGS detector and usage of Smart Orbit single bounce diamond ATR accessory (SibFU CEJU). The spectrum of each sample was recorded by accumulating 32 scans at  $4 \text{ cm}^{-1}$  resolution between  $400$  and  $4000 \text{ cm}^{-1}$ . Investigation was held for initial ATC and samples, which were annealed at  $375$ ,  $430$ ,  $470$ ,  $600 \text{ K}$ . Choice of temperatures is based on TGA result (Fig. 4a). Concern to this, mass loss during the annealing time of each sample corresponds to mass loss results of TGA.

## 3. Results and discussion

Under normal conditions, the obtained aluminum chloride acid solution is a limpid glutinous yellowy liquid. The solution density is  $1.33 \text{ g/cm}^3$ , which is close to the published data for a saturated aluminum chloride solution that has a density of  $1.35 \text{ g/cm}^3$  with an  $\text{AlCl}_3$  content of approximately  $41 \text{ wt}\%$  [8]. The Al:Cl weight ratio (in the dried solid sample) obtained with XRD is approximately  $16:84$ , and the atomic ratio is  $1:4$  (drying occurred under  $300 \text{ K}$ ). Simultaneously, the Al:Cl weight ratio for  $\text{AlCl}_3$  is  $20:80$  (atomic ratio is  $1:3$ ). This result demonstrates the excess of hydrochloric acid in the solution. One mol of trichloride has already been found to correspond to approximately 1 mol of hydrochloric acid. The  $\text{pH} = -0.72$ , and all of the results described above support the existence of chloride complexes in the solution, which are

typical for  $\text{HAICl}_4$  super acids derived from Lewis acids ( $\text{AlCl}_3$ ) and Bronsted protonic acids ( $\text{HCl}$ ) [9,10]:



As a result of the isothermal heat treatments of aluminum trichloride in open air at temperatures of  $423$ ,  $448$ ,  $473$ ,  $573$ ,  $873$ ,  $1073$ ,  $1223$ ,  $1323$  and  $1423 \text{ K}$  for  $20 \text{ h}$ , it was observed that the mass of the sample stabilizes at  $32\%$  of the initial mass under  $423 \text{ K}$ . The solid residue was yellow plate-like particles with hygroscopic properties. Further thermal treatment at temperatures less than  $573 \text{ K}$  leads to the residual matter of  $13.5\%$  in the form of a white, but not hygroscopic, powder. The following stages of the heat treatment slightly changed the mass of the sample –  $13.1\%$  (Fig. 1). Thus, the general processes of water evaporation and thermal decomposition with a release of volatile products during the long-term isothermal treatment practically stops up to the temperature of  $570 \text{ K}$ .

Isothermal drying of the aluminum trichloride solution under a temperature of  $373 \text{ K}$  leads to an approximate  $52\%$  weight loss in comparison with  $5\text{--}7\%$ , as the thermogram showed in Fig. 4. Drying occurs with the fast formation of a solid, dense film of salt on the surface of the solution, and the evaporation practically stops. It takes  $5\text{--}7$  days to obtain yellow crystals when the film cracked regularly. XRF analysis revealed that the Al:Cl atomic ratio in this product is approximately  $1:3$ . Furthermore, the XRD analysis identified the general phase, which is aluminum trichloride hydrate ( $\text{AlCl}_3 \cdot 6\text{H}_2\text{O}$ ). As the temperature increases to  $423 \text{ K}$ , the formation of a salt film does not occur. After  $20 \text{ h}$  of heat treatment, the sample loses approximately  $68\%$  of weight (Fig. 1) in comparison with  $43\%$ , as the thermogram showed (Fig. 4). Once the Al:Cl atomic ratio in the product becomes equal to  $1:1.65$ , its total composition can be evaluated as  $\text{Al}_2\text{O}_3 \cdot 3, 3\text{HCl} \cdot \text{H}_2\text{O}$ . When the conditions are close to equilibrium, the substance loses more than one-half of chlorine, even under  $423 \text{ K}$ , whereas the thermogram only shows the beginning of this process under the same conditions, and it reaches the same level when the sample is overheated by  $40\text{--}50 \text{ K}$ . Similar results are observed for higher temperatures:  $448 \text{ K}$  – Al:Cl (atomic ratio) =  $1:0.7$  ( $\text{Al}_2\text{O}_3 \cdot$

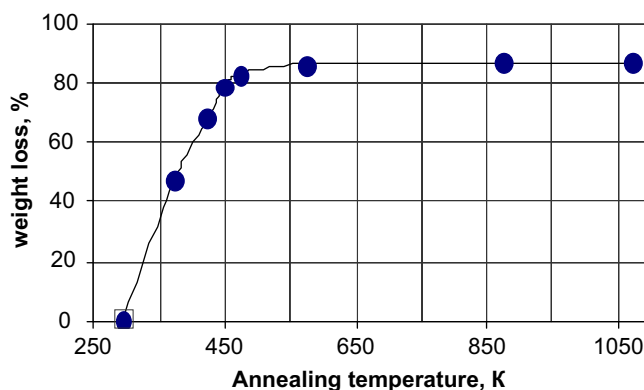


Fig. 1. Aluminum trichloride sample weight loss under isothermal annealing.

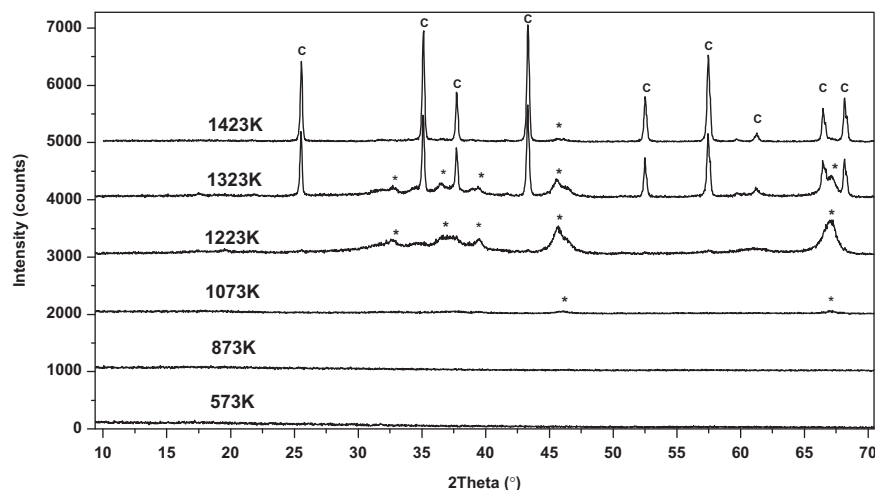


Fig. 2. X-ray powder patterns of thermolysis products at different temperatures; \* – peaks of  $\gamma$ - $\text{Al}_2\text{O}_3$ , C –  $\alpha$ - $\text{Al}_2\text{O}_3$ .

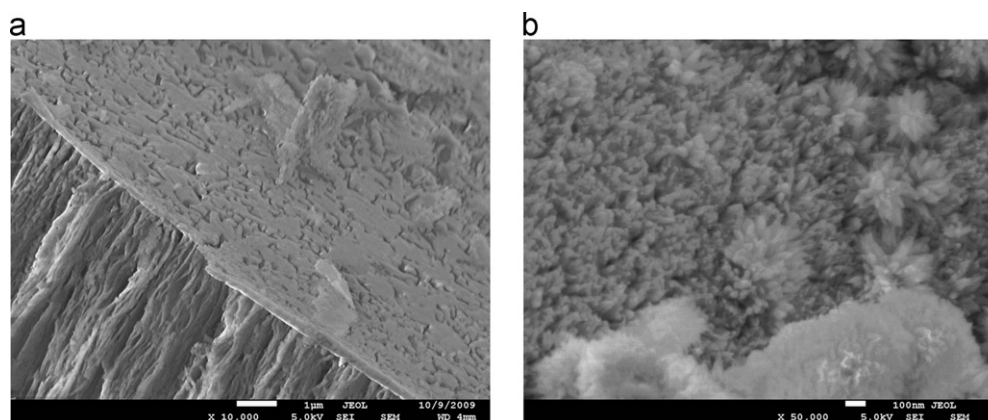


Fig. 3. SEM images of the final thermolysis products: (a)  $\alpha$ - $\text{Al}_2\text{O}_3$  after sintering at 1423 K, (b) –  $\gamma$ - $\text{Al}_2\text{O}_3$  on  $\text{TiB}_2$  as a substrate after 2 h at 1123 K.

$1.4\text{HCl} \cdot 0.2 \text{ 6H}_2\text{O}$ ), 473 K –  $\text{Al}:\text{Cl}$  (atomic ratio)=1:0.5 ( $\text{Al}_2\text{O}_3 \cdot \text{HCl} \cdot 0.1\text{H}_2\text{O}$ ). The water quantity in the total composition expressions can be calculated as a large number difference, and therefore, it can be substantially underestimated when the  $\text{Al}:\text{Cl}$  ratio is determined, even for small error (the error is no more than 5%).

The X-ray powder diffraction patterns of the samples after each stage of annealing are shown in Fig. 2. The typical SEM images of the powder microstructure are presented in Fig. 3. The matter is amorphous at temperature less than 1073 K, despite the data in the literature on the crystallization of  $\text{Al}(\text{OH})_3$  amorphous gels during aging or weak heating [1]. Weak peaks appear at 1073 K, and the set of peaks that appeared at 1223 K allows us to reliably identify the  $\gamma$ - $\text{Al}_2\text{O}_3$ . The sample crystallizes at 1423 K to form corundum, which is in agreement with the data reported in [1].

The powder morphology is identical at all of the annealing temperatures. The powders are agglomerates of lamellar structures (Fig. 3a). The thicknesses of the plate-layers and the pore dimensions are nanoscale. As can be observed, the plate-like particles are the product of the

quasi-liquefied state. This process results in a particle that has a sufficiently smooth surface covered by pores. The initiation of the pores is likely caused by water rise onto the surface, which occurred because of substance decomposition into the particle volume. On the particle fracture, we can observe the morphology of the internal pores. The pores are of an extended nature that gives a fibrous type to the internal structure. It is obvious that the specific area of such powders is large. This result can be used when large dimensions of this characteristic are necessary.

Experiments, including long-term isothermal heat treatments, resulted in a practically equilibrium product. The results of such experiments are substantially different from the thermal study data. The set of aluminum trichloride solution thermal decomposition characteristic properties were revealed during the kinetic experiments in the low-temperature range (Fig. 4). General dehydration and decomposition processes occur up to 550–600 K. The TG curves have a complicated form with some specific sections of sample weight decrease. The DSC curves with a set of consistent endothermic peaks correspond to these TG dependences. The increased rate of heating up to 366 K

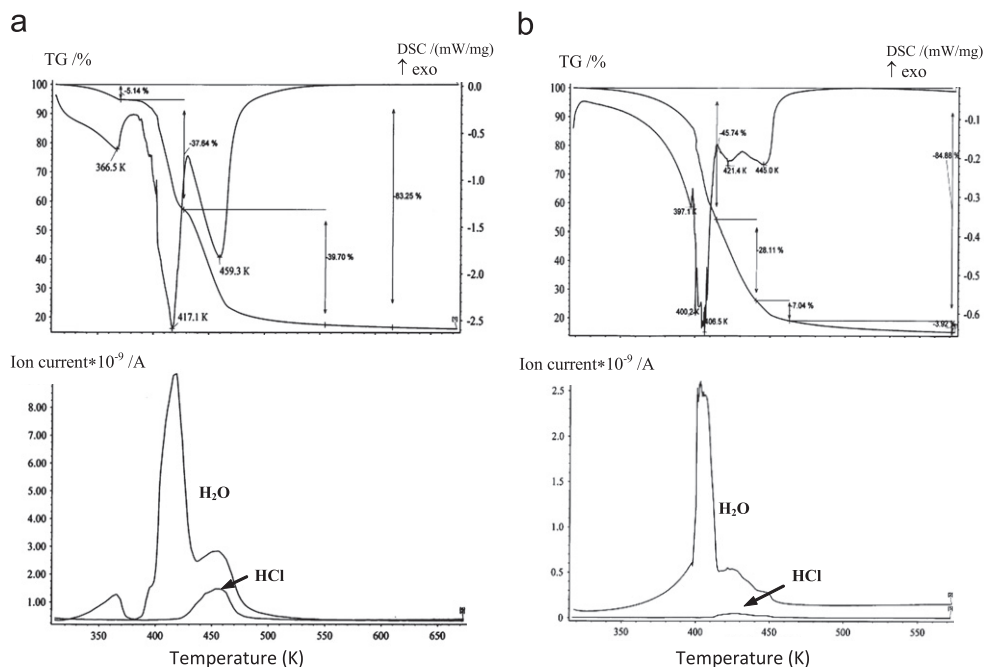


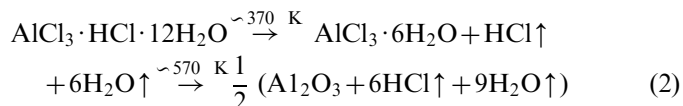
Fig. 4. TG, DSC and EMS curves of ATC heating for 5 (a) and 1 (b) K/min rates.

(Fig. 4a) results in a weight decrease of approximately 3–5%, which is accompanied by both a broad endothermic effect and an EMS-peak that arose from the free water evolving. The stepped weight change of 37.6% is accompanied by a substantial endothermic effect, a peak resulting from the free water evolving (peak max at 417 K), and the starting hydrogen chloride evolving between 390 and 440 K. A weight decrease of approximately 34% with substantial heat absorption and H<sub>2</sub>O and HCl release occurs between 440 and 470 K. However, the DSC peaks are caused by heat absorption, and the peaks of H<sub>2</sub>O and HCl release are related to the temperature of approximately 460 K. The water continues evolving at temperatures higher than 470 K up to 550 K. Substantially intensive chlorine hydride evolving occurs between 425 and 485 K. The track of ions with weight corresponded to molecular chlorine, which can also be observed in this temperature range. Upon reaching 600–650 K, the sample weight was 17% of the initial weight. The weight is appropriately less than that during the isothermal annealing. The thermogram obtained up to 1100 K shows a good agreement between the solid residue and the isothermal annealing products (13.07%).

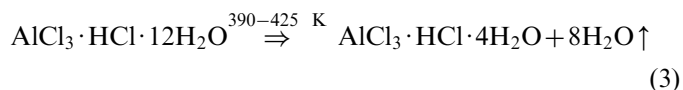
Dependencies obtained for the different heating rates are the same, and they have characteristic points that are substantially shifted to lower temperatures for heating rates of 1 K/min. Both the low-temperature range of these curves and the DSC peak splitting for 459 K are different for the described thermogram.

The chemical composition of the close to saturation ATC solution can be expressed in terms of the conditional balance formula  $\text{AlCl}_3 \cdot \text{HCl} \cdot 12\text{H}_2\text{O}$ . This formula was deduced from the XRF analysis data, pH of the solution

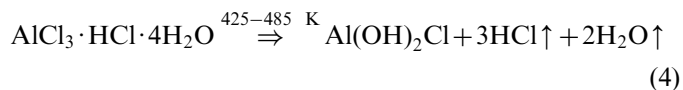
and the weight of the dried solid data, which was obtained from the long-time high-temperature annealing. The obtained substance thermally decomposes under very slow heating in accord with the total chemical equation:



When the rate of heating is comparatively large (5 K/min), the  $\text{AlCl}_3 \cdot \text{HCl} \cdot 12\text{H}_2\text{O}$  compound loses eight molecules of water during the first stage of decomposition (390–425 K):



The weight loss and the composition of the gases before HCl began releasing can be concluded from the data. The calculations from the TG and EMS curves indicate that the consequent heating for the temperature range of 425–485 K leads to the elimination of 3 HCl molecules and 2 H<sub>2</sub>O molecules with formation of  $\text{Al}(\text{OH})_2\text{Cl}$ :



When the heating temperature is increased to high values, the  $\text{Al}(\text{OH})_2\text{Cl}$  decomposition occurs and is accompanied by the slow elimination of water and HCl. The concentrations of H<sub>2</sub>O and HCl in the gas phase are likely too low to be detected using our equipment.

Inherently proposed reactions schemes of thermolysis rely on results of TGA and EMS investigations. The structural peculiarity of the formed compounds is not considered in



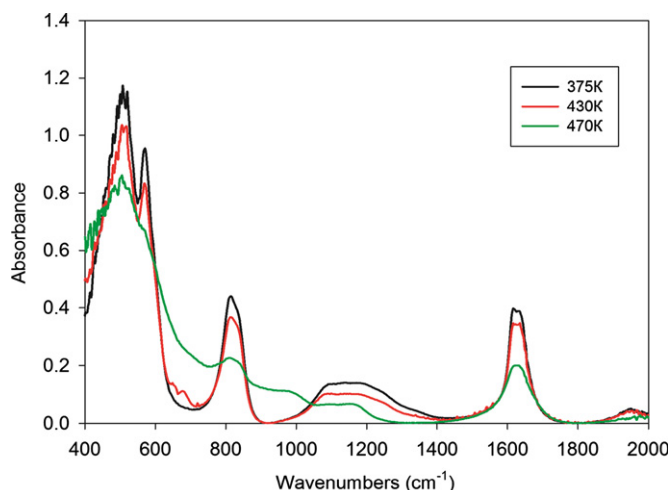


Fig. 5. IR spectra of ATC which was annealed at different temperatures.

this paper and need separate researches with involvement of complementary methods. Nevertheless, we can match the fact that with accordance to IR-spectroscopy investigation during annealing process, we can observe Al–Cl and Al–O modes.

The appearance of 500, 560 and 815  $\text{cm}^{-1}$  modes is observed at 375 and 430 K (Fig. 5). These lines don't take place in initial ATC IR-spectra because of a substantial water presence. The mode 500  $\text{cm}^{-1}$  concerns to Al–Cl [11] and 560  $\text{cm}^{-1}$  to Al–OH mode according to [12]. The mode at 815  $\text{cm}^{-1}$  may be define as stretching ( $\text{AlO}_6$ ) or ( $\text{AlO}_4$ ) [13]. To the extent of the annealing temperature enhancement up to 470 K and higher intensity of modes, which were noted before, are reduced. The same situation takes place for 1630  $\text{cm}^{-1}$  mode, which one corresponds to water. Appearance of reflexes and reducing of their intensity can be an evidence for processes (3) and (4).

It is obvious that both the described sequence of stages and the intermediate products have a very relative nature that is only approximately satisfied by the obtained TG and DSC curves. Moreover, it is necessary to take into account that these measurements do not relate with the equilibrium state and that the transformation temperature ranges depend on the increasing temperature rate. Indeed, the actual process is more complicated; at the different temperatures, the products could be mixtures with different basicity and watering. Nevertheless, such data are very interesting for the thermolysis process analysis of this binding material during the synthesis of ceramics and composite materials.

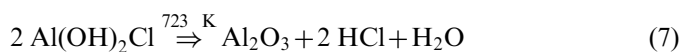
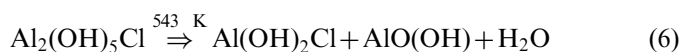
The thermolysis process of  $\text{AlCl}_3 \cdot 6\text{H}_2\text{O}$  leads to the formation of intermediate ( $\text{Al}_2(\text{OH})_5\text{Cl}$ ,  $\text{Al}(\text{OH})_2\text{Cl}$  etc.) compounds [2]. The decomposition products have an Al:Cl ratio of approximately 1.1–2.3. The mixture of hydrochlorides was identified during the isothermal treatment of  $\text{AlCl}_3 \cdot 6\text{H}_2\text{O}$  at 438 K [2]:



where:  $1 < x < 2$ ,  $y \approx 2$ . The slow heating of  $\text{AlCl}_3 \cdot 6\text{H}_2\text{O}$  up to 543 K [3] leads to the formation of the water

soluble basic chloride  $\text{Al}_2\text{O}_3 \cdot 2\text{HCl} \cdot 2\text{H}_2\text{O}$  (or  $\text{Al}(\text{OH})_2\text{Cl} \cdot 0,5\text{H}_2\text{O}$ ). These coefficients appropriately exceed both the data from [2] and our results from the isothermal heat treatments.

The thermal transformations of the hydroxychlorides also are presented by means of the scheme where the hydroxychlorides are appropriately more stable with greater basicity at low temperatures:



Here, the temperature range of 473–723 K is presented for total decomposition equation of full  $\text{AlCl}_3 \cdot 6\text{H}_2\text{O}$  to aluminum oxide.

The complicated thermolysis process of aluminum trichloride through the formation of intermediate hydroxychlorides is described in strikingly different ways. These processes are likely caused by the differences in the heating rates of the samples, samples prehistory, and the amount and nature of the impurities. The results of the ATC decomposition for the kinetic experimental conditions during the thermal analysis are obtained in the present work, and there is good agreement between our results and the results from other works for preparative trichloride  $\text{AlCl}_3 \cdot 6\text{H}_2\text{O}$  thermolysis.

By comparing the data obtained from ATC, it is necessary to conclude that the processes that take place under the studied solution heating substantially depend on the heating rate, and these processes can be presented as the set of transformations that included free water evaporation, step-by-step crystalline water dehydration, trichloride hydrolysis due to crystalline water, HCl elimination, residual water and HCl gradual elimination up to 1300 K with chemical crystal transformation.

#### 4. ATC application

It is well known that solutions of aluminum trichloride and hydroxychlorides as well as aluminum trichloride thermolysis intermediate products have the properties of low-temperature bands and high-temperature cements for engineering applications during the production of ceramics and mineral composites. An ATC solution in the described nature was tested for composite materials on basis of titanium diboride  $\text{TiB}_2/\text{Al}_2\text{O}_3$ .  $\text{TiB}_2$ – $\text{Al}_2\text{O}_3$ –ATC compositions with various  $\text{TiB}_2$  and  $\text{Al}_2\text{O}_3$  powder ratios and ATC contents within 2–10 wt% were mixed thoroughly. The samples were molded by pressing. After air drying (473 K) and sintering (1123 K, for 2 h in a closed container under the carbonic fill), the materials had a compression strength of 20–100 MPa with a relative density of 0.58–0.62. In all cases, the technological stability of “young” stock materials was demonstrated. This result confirms the adhesive capacity of ATC in contrast to aluminum trichloride solutions. In Fig. 3(b), the SEM image shows the microstructure of aluminum oxide obtained from

ATC on the  $\text{TiB}_2$  substrate. Evenly deposited aluminum oxide created a surface coating with needle-shaped dendrites that had branch lengths less than 100 nm. The large specific surface is responsible for the high binding property. The solutions of hydroxychlorides, which are the products of  $\text{Al}(\text{OH})_3$  and  $\text{HCl}$  reaction or half-way  $\text{AlCl}_3 \cdot 6\text{H}_2\text{O}$  thermolysis, also have the adhesive capacity of the low-temperature band. However, such bands are poorly applicable because of substantial viscosity, low aluminum content, and short time stability. The ATC solution is free from all shortcomings described above, and it has unlimited time stability because four years of storage did not reveal any change.

## 5. Conclusions

The close to saturation acidic solution of aluminum trichloride with the general formula  $\text{AlCl}_3 \cdot \text{HCl} \cdot 12\text{H}_2\text{O}$  has both low-temperature bands and high-temperature cement properties during the preparation of some composite powdered materials, specifically based on titanium diboride and aluminum oxide. The thermolysis processes of such solutions substantially depend on the heating rate. These processes occur through the formation of intermediate hydroxychlorides and stop at approximately 570 K, which is similar to that for the  $\text{AlCl}_3 \cdot 6\text{H}_2\text{O}$  salt decomposition. Isothermal drying at  $\sim 370$  K results in the formation of  $\text{AlCl}_3 \cdot 6\text{H}_2\text{O}$ . Crystals of  $\gamma\text{-Al}_2\text{O}_3$  begin to appear at 1073 K, and then, the  $\alpha\text{-Al}_2\text{O}_3$  final product forms at 1323 K. Moreover,  $\gamma\text{-Al}_2\text{O}_3$  can be promising as catalyst supports for the active phase in heterogeneous catalysis because of the high specific surface area in  $\gamma\text{-Al}_2\text{O}_3$  that was prepared by heat treatments at approximately 1220 K.

## Acknowledgments

This work has been performed under 2.1.2/780 project of analytic departmental special-purpose programme “High school scientific potential development (2009–2010) and

State contract no. 02.740.11.0269 (the Ministry of Education and Science Russian Federation)”

## References

- [1] Charles N. Satterfield, *Heterogeneous catalysis in practice*, McGraw-Hill, 1980.
- [2] D. Petzold, R. Naumann, Thermoanalytische Untersuchungen zur Bildung kristalliner  $\text{Al}_2\text{O}_3$ -Formen bei der thermischen Zersetzung von Aluminiumchloridhexahydrate, *Journal of Thermal Analysis* 20 (1981) 71–86, <http://dx.doi.org/10.1007/BF01912998>.
- [3] M. Hartman, O. Trnka, O. Šolcová, Thermal Decomposition of Aluminum Chloride Hexahydrate, *Industrial and Engineering Chemistry Research* 44 (2005) 6591–6598, <http://dx.doi.org/10.1021/ie058005y>.
- [4] D.R. Buchanan, P.M. Harris, A neutron and X-ray diffraction investigation of aluminum chloride hexahydrate, *Acta Crystallographica B* 24 (1968) 954–960, <http://dx.doi.org/10.1107/S056774086800347X>.
- [5] S. Sikorska, S. Freza, P. Skurski, The reason why  $\text{HAlCl}_4$  acid does not exist, *Journal of Physical Chemistry A* 114 (2010) 2235–2239, <http://dx.doi.org/10.1021/jp910589m>.
- [6] E. Perenthaler, H. Schulz, A. Rabenau, Die strukturen von  $\text{LiAlCl}_4$  und  $\text{NaAlCl}_4$  als funktion der temperatur, *Zeitschrift für anorganische und allgemeine Chemie* 491 (1982) 259–265, <http://dx.doi.org/10.1002/zaac.19824910133>.
- [7] B. Krebs, H. Greiwing, C. Brendel, F. Taulelle, M. Gaune-Escard, R.W. Berg, Crystallographic and aluminum-27 NMR study on premelting phenomena in crystals of sodium tetrachloroaluminate, *Inorganic Chemistry* 30 (1991) 981–988, <http://dx.doi.org/10.1021/ic00005a021>.
- [8] J.W. Mellor, *A Comprehensive Treatise on Inorganic and Theoretical Chemistry*, London – New York – Toronto, V.5, 1929.
- [9] Norris F. Hall, James B. Conant, A study of superacid solutions. i. the use of the chloranil electrode in glacial acetic acid and the strength of certain weak bases, *Journal of the American Chemical Society* 49 (1927) 3047–3061, <http://dx.doi.org/10.1021/ja01411a010>.
- [10] W.D. Chandler, K.E. Johnson, Thermodynamic Calculations for reactions involving hydrogen halide polymers, ions, and lewis acid adducts. 3. systems constituted from  $\text{Al}^{3+}$ ,  $\text{H}^+$ , and  $\text{Cl}^-$ , *Inorganic Chemistry* 38 (1999) 2050–2056, <http://dx.doi.org/10.1021/ic980640r>.
- [11] Kazuo Nakamoto, *Infrared and Raman Spectra of Inorganic and Coordination Compounds*, Fourth Edition, Wiley, John & Sons, Incorporated, New York, 1986.
- [12] Theo J. Klopogge, Ray L. Frost, Leisel Hickey, FT-Raman and FT-IR spectroscopic study of the local structure of synthetic Mg/Zn/Al-hydroxalclites, *Journal of Raman Spectroscopy* 35 (2004) 967–974.
- [13] S. Rana, S. Ram, Self-controlled growth in highly stable  $\alpha\text{-Al}_2\text{O}_3$  nanoparticles in mesoporous structure, *Physica Status Solidi (A)* 201 (2004) 427–444, <http://dx.doi.org/10.1002/pssa.200306729>.